JOURNAL OF MATERIALS SCIENCE **41** (2006) 87–96

Studies on the relaxor behavior of sol-gel derived $Ba(Zr_xTi_{1-x})O_3$ ($0.30 \leq x \leq 0.70$) thin films

A. DIXIT, S. B. MAJUMDER, R. S. KATIYAR*
Department of Physics, University of Puerto Rico, San Juan, PR 00931-3343
E-mail: rkatiyar@rrpac.upr.clu.edu

A. S. BHALLA
Materials Research Laboratory, Pennsylvania State University, University Park, PA 16802

We have studied the relaxor behavior of sol-gel derived $Ba(Zr_xTi_{1-x})O_3$ ($0.30 \leq x \leq 0.70$) thin films. The plausible mechanism of the relaxor behavior has been analyzed from the dielectric data and micro-Raman spectra. Substitution of Zr^{+4} for Ti^{+4} in $BaTiO_3$ lattice reduces its long-range polarization order yielding a diffused paraelectric to ferroelectric phase transition. The solid solution system is visualized as a mixture of Ti^{+4} rich polar region and Zr^{+4} rich regions and with the increase in Zr contents the volume fraction of the polar regions are progressively reduced. At about 25.0 at% Zr contents the polar regions exhibit typical relaxor behavior. The degree of relaxation increases with Zr content and maximizes at 40.0 at% Zr doped film. The frequency dependence of the polar regions follows Vogel-Fulcher relation with a characteristic cooperative freezing at freezing temperature (T_f). Below T_f, a long range polarization ordering was ascertained from the polarization hysteresis measurement.

1. Introduction

Relaxors exhibit unusually higher dielectric constant and piezoelectric constants, which are very attractive for high energy density capacitors and actuators. Lead based perovskite ceramics has been extensively studied in last couple of decades. Studies on relaxors in thin film form are scanty and the available reports mostly are based on lead based perovskite thin films. These relaxor, irrespective in bulk ceramics or thin film forms have the following general characteristics: (i) all of them exhibit a diffuse phase transition (DPT) like behavior, where the temperature corresponding to the dielectric maxima (T_m) does not correspond any paraelectric-ferroelectric phase transition like normal ferroelectrics, (ii) T_m shifts to higher temperature with the increase in measurement frequency, (iii) a frequency dispersive behavior is also observed in the dielectric loss tangent, however, the peak temperatures (T'_m) for dielectric loss do not coincide with the corresponding T_m (iv) relaxors follow the Curie-Weiss law far above T_m, (iv) if the temperature is significantly lowered as compared to T_m, some of these relaxors exhibit stable polarization hysteresis.

The classic ferroelectric relaxors are $A(B'_xB''_{1-x})O_3$ (e.g. $Pb(Mg_{1/3}Nb_{2/3})O_3$) type complex compounds where the nano-size cation ordered polar regions, distributed in a disordered matrix, are known to be responsible for their relaxor behavior. Several model has been proposed to explain the relaxor behavior in PMN ceramics which includes a super-paraelectric model [1], glass-like freezing of the nano-polar regions [2], random field model [3] involving the occurrence of dynamic nanopolar regions in the paraelectric phase and their transformation into frozen domain upon cooling below the freezing temperature etc. Relaxor behavior is also reported in tetragonal tungsten bronze type compounds, doped quantum paraelectrics, *A* and *B* site doped perovskite oxides [4, 5] etc.

Recently, the attention has moved towards barium based relaxors as these are environmentally friendly lead free oxides. From the studies on the bulk ceramics and single

---

*Author to whom all correspondence should be addressed.

0022-2461 © *2006 Springer Science + Business Media, Inc.*
DOI: 10.1007/s10853-005-5929-1

crystalline barium zirconate titanate it is apparent that the Zr contents strongly affect the ferroelectric, piezoelectric, dielectric as well as relaxor characteristics of BZT ceramics [6–8]. We have already reported the relaxor characteristics in $BaZr_{0.40}Ti_{0.60}O_3$ (BZT-40) thin films, which has also been confirmed later by others, however, the mechanism lead to the observed relaxor behavior so far remain poorly understood even in case of bulk BZT ceramics [6, 9, 10]. The available literature reports are contradictory in nature as apparent from the following review. Sciau *et al.* reported that unlike $PbMg_{1/3}Nb_{2/3}O_3$ (PMN), $BaZr_{0.35}Ti_{0.65}O_3$ (BZT-35) does not have any cation ordered regions and the loss of the polar ordering of $BaTiO_3$ is due to the dilution of Ti^{+4} ions by Zr^{+4} substitution. The same group has also reported that, as observed in case of PMN ceramics, the application of external electric field does not induce any long-range polar order in BZT ceramics due to the difficulty of polarizing the Zr rich regions [11, 12]. In contrary to these reports, from the measurement of pyroelectric current, Farhi *et al.* [13] claimed that a field induced ferroelectric phase can be stabilized below the freezing temperature of $BaZr_{0.40}Ti_{0.60}O_3$ (BZT-40) ceramics. The freezing temperature was estimated to be in the range of 100–140 K from dielectric, Raman and pyro-current measurements and it represent to ergodic to non-ergodic phase transition. Apparently, in a solid solution system like BZT, no cationic ordering is expected between Zr and Ti. In several relaxor compounds (viz. PMN, PST etc.), cationic order of B site ions has been confirmed to be related to the dielectric relaxation. Artificial control of *B* site cation ordering has been demonstrated to be possible by constructing superlattices, however, from this report the relaxor characteristics of $BaZr_{0.20}Ti_{0.80}O_3$ (BZT-20) thin films with different degree of cation ordering are not properly elucidated [14].

In the present work we have prepared BZT thin films with Zr content varies from 30.0–70.0 at%. To the best of our knowledge no attempt has so far been made to study the dielectric behavior of BZT ceramics or thin films with Zr contents more than 40.0 at%. The relaxor behavior of BZT thin films were confirmed in the whole range of Zr contents. The dielectric relaxations in these films found to follow the Vogel-Fulcher type behavior originally reported for the spin-glass as well as complex perovskite systems and below a characteristics freezing temperature relaxor to ferroelectric transition has been demonstrated. Based on the dielectric, ferroelectric and micro-Raman scattering analyses, the observed relaxor behavior has been hypothesized due to the breakdown of the long range polar ordering in $BaTiO_3$ (BTO) by Zr^{+4} substitution in Ti^{+4} sites yielding a nano-size polar regions in a Zr rich matrix. Beyond an optimal dopant content ($\geq$25.0 at%) probably a critical size of the polar regions are reached to yield the relaxor behavior of BZT thin films.

2. Experimental

In the present work, we present a comprehensive study to support the relaxor like behavior in $BaZr_xTi_{1-x}O_3$ ($0.30 \leq x \leq 0.70$) thin films prepared on platinum substrates by the sol-gel technique. Details of the precursor sol preparation have been reported elsewhere [15]. As deposited films were fired at 600°C for 5 min. for organic removal and initial crystallization. The coating and firing sequence was repeated for 20 times to attain a film thickness of about 600 nm. The films were finally annealed at 1100°C for 2 h in air for complete perovskite phase formation and better crystallinity. Polycrystalline perovskite nature of films was investigated using the X-ray diffraction method.

To measure the electrical properties circular Pt electrodes of 0.2 mm diameters were deposited on BZT films by dc magnetron sputtering. Electrical measurements and temperature dependent dielectric properties were studied in metal-insulator-metal configuration and the films were characterized using an impedance analyzer (HP 4294A, from Agilent Technology Inc.) in conjunction with a temperature controlled probe station (MMR Technology). The Polarization hysteresis nature of the film was analyzed using a ferroelectric tester system RT-6000 HVS from Radiant Technologies Inc. Raman spectra of these films were recorded using an ISA T64000 Raman microprobe. An optical microscope with 80 X objective was used to focus the 514.5 nm radiation from a Coherent Innova 99 Ar^+ laser on the sample. The same microscope objective was used to collect the backscattered radiation. The scattered light collected by the microscope and dispersed by the spectrometer was detected by a charge-coupled device (CCD) detection system. With 1″ CCD and 1800 grooves/mm grating, the spectral resolution was typically less than 1 cm^{-1}.

3. Results and discussions

3.1. Dielectric behavior

The temperature dependent capacitance and loss tangent of $Ba(Zr_xTi_{1-x})O_3$ ($0.30 \leq x \leq 0.70$) thin films were measured in a frequency range of 10 kHz-1 MHz using an impedance bridge and computer controlled thermal stage probe station. Fig. 1 shows the temperature dependent (a) dielectric constant (K) and (b) loss tangent ($\tan\delta$) of $Ba(Zr_{0.40}Ti_{0.60})O_3$, measured in a frequency range from 1 KHz to 1 MHz. A broad dielectric anomaly is apparent both in dielectric constant and loss tangent plots; however, the temperatures correspond to the dielectric constant maxima (T_m) do not coincide to that of the corresponding loss tangent maxima (T_m'). Both T_m as well as T_m' shift to higher temperature with the increase in frequency. For the other thin film compositions, similar features were observed in the temperature dependent dielectric constant and loss tangent behaviors as a function of frequencies;

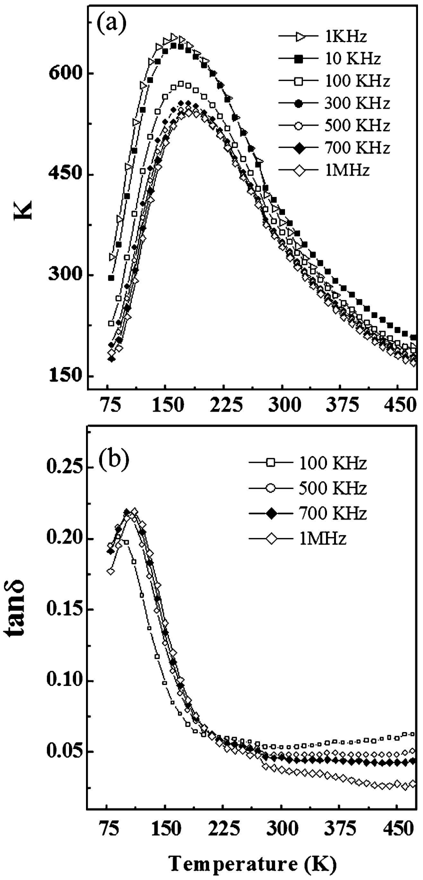

Figure 1 Temperature variation of (a) dielectric constant and (b) loss tangent of $Ba(Zr_{0.40}Ti_{0.60})O_3$ thin film measured in a frequency range of 1 kHz to 1 MHz.

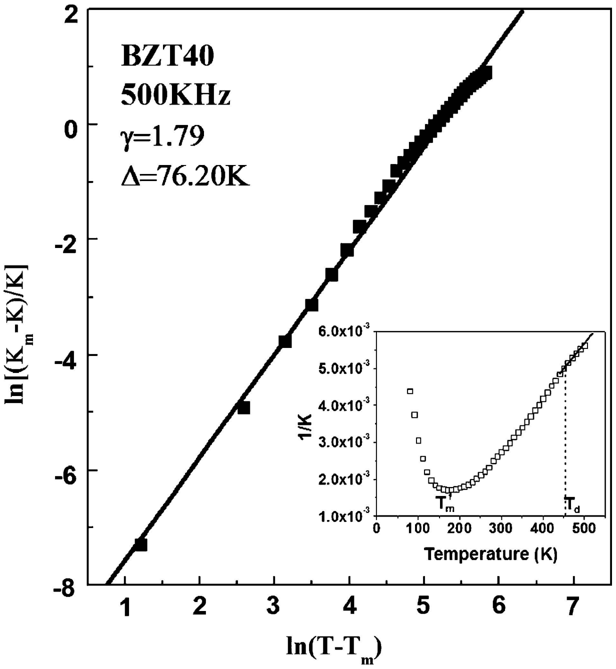

Figure 2 Plot of ln[(K_m−K)/K] vs. ln (T−T_m) for $Ba(Zr_{0.40}Ti_{0.60})O_3$ thin films. The symbols represents experimental data and the solid line fitted according to Equation 1. The inset shows the plot of 1/K vs. T for $Ba(Zr_{0.40}Ti_{0.60})O_3$ thin film. The solid line, fitted according to the Curie-Weiss law ($1/K = (T-\theta)/C$, C is the Curie constant, θ is the Curie-Weiss temperature) is valid far above T_m (see text).

however, a systematic decrease of T_m was observed with the increase in Zr contents varied from 30.0 to 70.0 at%. From the observed frequency dependence of the dielectric response it is imperative that in the composition range $0.30 \leq x \leq 0.70$, $Ba(Zr_xTi_{1-x})O_3$ thin films exhibit typical relaxor behavior with the estimated dielectric constant decreases and T_m shifts to higher temperature with the increase in measurement frequencies.

One of the main features of the phase transition in relaxor ferroelectrics in general, is the broadening of the transition termed as diffuse phase transition (DPT). In the vicinity of the broadening of dielectric maxima, the temperature variation of dielectric constant (K) is known to follow a power relation [16]:

$$1/K(f, T) = 1/K_m(f)\{1 + [T - T_m(f)]^{\gamma}/2\Delta^2\} \quad (1)$$

where K is the dielectric constant, K_m is the peak dielectric constant, T is the temperature, T_m is the peak temperature corresponding to the dielectric constant maxima, γ is the degree of relaxation, and Δ is the broadening parameter. From the linear fit between ln[(K_m/K)−1] vs ln (T−T_m) we have estimated the values of γ (from slope) and Δ (from intercept) as a function of frequencies for BZT thin films with Zr contents in the range of 30.0 to 70.0 at%. Fig. 2 shows such a typical linear fit for $Ba(Zr_{0.40}Ti_{0.60})O_3$ thin films measured at 500 kHz and the estimated values of γ and Δ for various Zr contents are 1.79 and 76°K respectively. From reported literature, the value of γ is equal to 2 for a perfect relaxor material, whereas for a perfect ferroelectric $\gamma = 1$ and Equation 1 reduced to Curie-Weiss law [6]. As shown in the inset of Fig. 2 the dielectric constant of $Ba(Zr_{0.40}Ti_{0.60})O_3$ film follows the Curie–Weiss behavior at temperatures much higher than T_m. Although a certain degree of subjectivity arises from the choice of the region where the linear fitting is applied, "far" from the temperature T_m, the Curie-Weiss law is considered valid. Accordingly, the temperature (T_d) where K^{-1} (T) starts to deviate from the typical Curie–Weiss behavior (∼ 460 K for BZT-40 film), is often considered the onset of the dynamic behavior of local polarization and termed as Burns temperature [17]. Table I summarizes the values of γ, Δ, *and* T_m (at 500 kHz), for BZT thin films with various Zr contents.

It is apparent from Table I that with the increase in Zr contents there is a systematic decrease in Δ, and T_m, whereas the degree of relaxation is much more evident in $Ba(Zr_{0.40}Ti_{0.60})O_3$ thin film. Beyond T_d, BZT thin films are paraelectric, in other words it is the highest temperature below which one begins to detect a local polarization

TABLE I Summary of the fitting parameters of the dielectric anomaly of BZT thin films.

Composition	γ (500 kHz)	Δ (K) (500 kHz)	T_m (K) (100 kHz)
$Ba(Zr_{0.30}Ti_{0.70})O_3$	1.7	83	213
$Ba(Zr_{0.40}Ti_{0.60})O_3$	1.8	76	170
$Ba(Zr_{0.60}Ti_{0.40})O_3$	1.6	65	154
$Ba(Zr_{0.70}Ti_{0.30})O_3$	1.3	35	147

in nano regions [17]. T_m is only located in the temperature range where a continuous change in the polarization distribution from polar nano-regions to a polar clusters takes place. In this temperature range the local polarization direction is determined by a fixed arrangement of atoms and no cooperative coupling exists between individual polar nano-regions so that an externally applied electric field could reverse the local polarization. In other words, with the application of external electric field rapid orientation of dipole moments in these nano-regions takes place however, once the field is removed the orientation is lost. Usually relaxor behavior is associated with the disorder in the occupation of the equivalent positions by different ions. For example in case of classic relaxor $Pb(Mg_{1/2}Nb_{2/3})O_3$ it is the disorder in the occupation of Mg^{+2} and Nb^{+5} ions in the B site of ABO_3 perovskite lattice. On the other hand in case of $Pb_{1-x}La_x(Zr_yTi_{1-y})O_3$ relaxors, it is the disorder in A site (between Pb^{+2} and La^{+3} ions) that yield the observed relaxor behavior. In this respect, it is interesting to note that in $Ba(Zr_xTi_{1-x})O_3$ system, in spite of Zr and Ti are isovalent ions, beyond an optimal content of Zr it exhibits typical relaxor behavior. In any classic relaxor system, in the vicinity of T_m, number of nano-size polar-regions exist each of which has a net polarization (P_s). Each of these polar regions has characteristic relaxation time (τ) decided by the local field configuration in them and their characteristic size. As the size of the PR decreases the energy barrier that separates the switching its polarization states also decreases and when the barrier height becomes comparable to thermal energy (kT), the direction of P_s fluctuates with temperature [1, 4]. Viehland *et al.* [2] proposed that the short-range interactions between the PR control the fluctuation of P_s leading to it's freezing at a characteristics temperature. Like the spin glass systems the dielectric relaxation in relaxors can be described by the well-known Vogel-Fulcher relation [18]:

$$f = f_o \exp[-E_a/k_B(T_m - T_f) \quad (2)$$

where f is the measurement frequency, f_o is the pre-exponential factor, E_a is the activation energy for polarization fluctuations of an isolated cluster, k_B is the Boltzmann constant, T_m is the temperature corresponding to the dielectric maxima, and T_f is the static freezing temperature. From Equation 2 as T_m approaches the characteristic freezing temperature T_f, $f \to 0$, in other words the kinetics of polarization fluctuation becomes extremely sluggish. From the frequency dependent (10 kHz to 1 MHz) dielectric anomaly we estimated the T_m and corresponding frequency (*f*) for all relaxor BZT thin films with different Zr contents. The data were fitted according to Vogel Fulcher relation (Equation 2) using a non-linear curve-fitting program and the parameters f_o, E_a, and T_f were extracted as a function of Zr contents. Fig. 3 shows the experimental data and the fitted line for BZT-40 thin film. Similar fitting was performed for other BZT compositions and the results are tabulated in Table II. For all the BZT thin film compositions in this study, a remarkable fit of the experimental data with the Vogel-Fulcher relation, suggests that the observed relaxor behavior is analogous to a spin glass system with polarization fluctuation above the static freezing temperature T_f. As shown in Table II, within the fitting error, it seems that the freezing temperature (T_f) reduces with the increase in Zr contents whereas the activation energy reduces in the range of 20–30 meV in the films with higher Zr contents (60.0–70.0 at%).

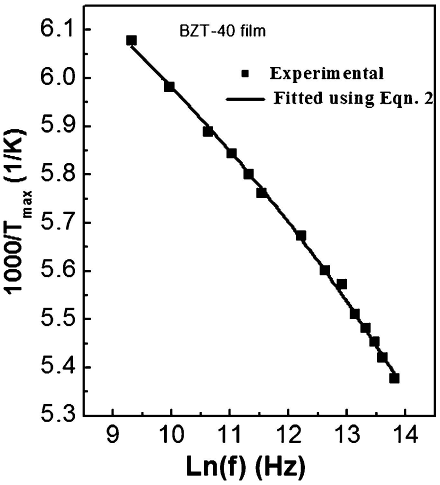

Figure 3 Variation of the inverse of T_m of $Ba(Zr_{0.40}Ti_{0.60})O_3$ thin film with frequency. The solid line is fitted according to the Vogel-Fulcher equation (see text).

TABLE II Summary of the Vogel-Fulcher fitting parameters of BZT thin films

Composition	Freezing temperature (T_f) (K)	Activation energy (E_a) (eV)	Pre-exponential factor (f_o) (Hz)
$Ba(Zr_{0.30}Ti_{0.70})O_3$	151(±13)	0.05 (±0.002)	0.036×10^{10}
$Ba(Zr_{0.40}Ti_{0.60})O_3$	118(±7)	0.06 (±0.005)	2.69×10^{10}
$Ba(Zr_{0.60}Ti_{0.40})O_3$	121(±4)	0.02 (±0.004)	0.01×10^{10}
$Ba(Zr_{0.70}Ti_{0.30})O_3$	94(±5)	0.03 (±0.006)	0.015×10^{10}

3.2. Micro-Raman scattering

From the dielectric studies of BZT single crystals it has been reported that on heating the rhombohedral to orthorhombic (T_2) and orthorhombic to tetragonal (T_3) transition temperatures of $BaTiO_3$ is increased whereas the Curie temperature (T_c) (tetragonal to cubic phase transition) is decreased with the increase in Zr content. All these three transition temperatures merge at about 15 at% Zr contents and the transition temperature decreases with further increase in Zr contents. Based on these studies a tentative phase diagram of $Ba(Zr_xTi_{1-x})O_3$ (up to $x \leq 0.2$) has been constructed which indicates that at room temperature $Ba(Zr_{0.20}Ti_{0.80})O_3$ has rhombohedral crystal structure [8]. The structural modification of BTO thin films doped with various Zr contents was investigated by micro-Raman scattering measurements and as reported in our earlier works [19], up to 10.0 at% Zr doped BTO films, the following facts can be ascertained from the temperature dependent Raman spectra, (i) the cubic-tetragonal transition temperature (T_c) progressively reduces with the increase in Zr contents, (ii) the tetragonal to orthorhombic transition temperature remains difficult to identify from the measured spectra, and (iii) the tetragonal (orthorhombic) to rhombohedral transition temperatures increase with increased Zr contents. Unlike the corresponding bulk compositions, the characteristic phase transition temperatures could not be identified from temperature dependent capacitance measurements of the respective thin film samples due to the very broad nature of dielectric anomaly. Beyond 10.0 at% Zr doping, the low temperature (77 K) phase is rhombohedral, with the increase in measurement temperature; no further phase transition could be detected. As for example in case of 20.0 at% Zr doped BTO thin films we have observed a frequency independent broad dielectric anomaly with the temperature corresponding the dielectric constant maxima is around 260 K (data not shown). The structural evolution of this film is elucidated in the temperature dependent Raman spectra (Fig. 4a). The anti-resonant mode about 125 cm^{-1} has been associated to the vibration of Zr ions in oxygen cage [13]. The low temperature (77 K) phase is identified rhombohedral, and also it is interesting to note that even at high temperature almost all the modes related to the rhombohedral structure are present although the intensities are reduced and the FWHM are increased with temperature. In case of $BaTiO_3$ thin film we observed the existence of second order Raman peaks beyond the transition temperature, which indicates a disordered cubic structure. This could be due to the fact that even above transition temperature Ti^{+4} ions do not assume the octahedral position of the perfect ABO_3 unit cell. However, the fact that all the modes in case of BZT-20 films remain relative sharp and intense (as compared to $BaTiO_3$), it clearly indicates that far above the temperature corresponding to the dielectric maxima (T_m) the thin film retains its low temperature rhombohedral structure. In case of $Ba(Zr_{0.40}Ti_{0.60})O_3$ thin films the observed modes are due to rhombohedral crystal structure at all temperature ranges (Fig. 4b). The relatively sharper modes irrespective of the temperature of measurements are indicative of polar nano-size regions in these thin films [20]. A plateau is observed in the high frequency region which consists an extra mode at ~780 cm^{-1} (marked by small arrow in Fig. 4b) in addition to the $A_1(LO_3)$ line at 720 cm^{-1}. The appearance of

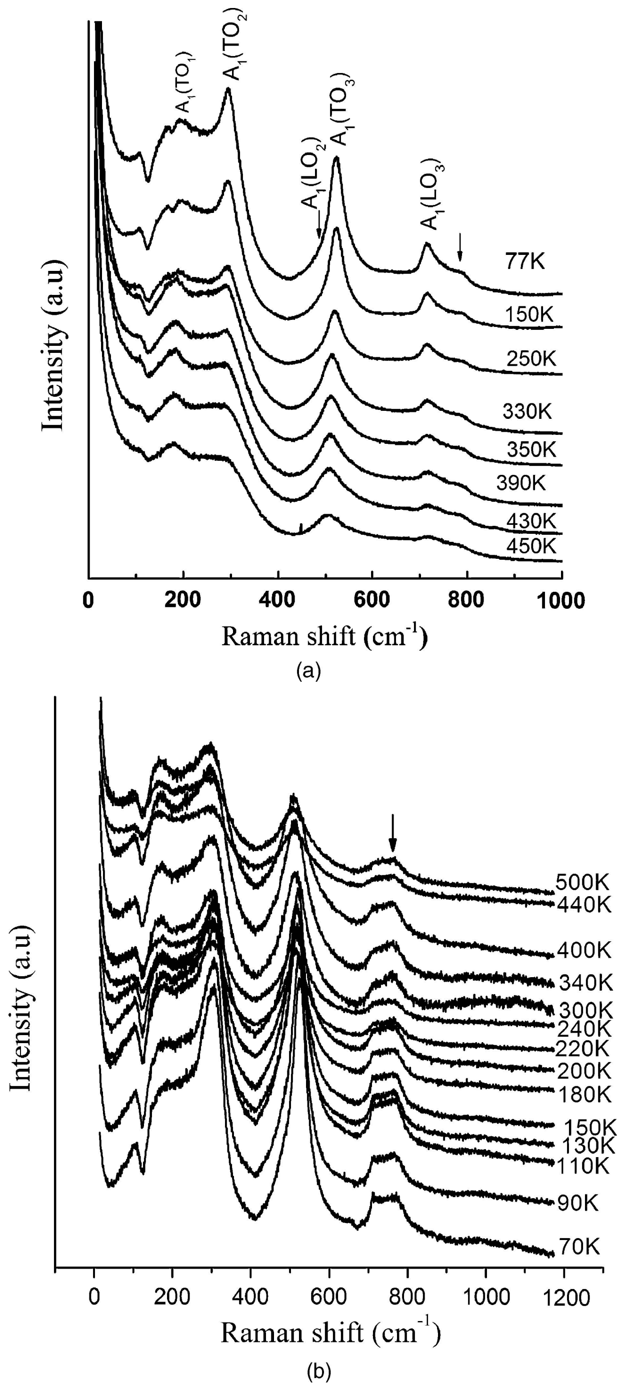

(a)

(b)

Figure 4 Temperature variation of the micro-Raman spectra of (a) $Ba(Zr_{0.20}Ti_{0.80})O_3$ and (b) $Ba(Zr_{0.40}Ti_{0.60})O_3$ thin films.

such plateau has been correlated with the relaxor nature of BZT ceramics [13]. As presented in the previous section, from the dielectric measurements, we have observed that BZT-20 film exhibits a typical diffuse phase transition behavior (plateau was indistinct) whereas the relaxor nature was distinctly confirmed in 25.0, 30.0 and 40.0 at% Zr doped thin films where the plateau became progressively well developed in the respective Raman spectra.

4. Discussions

The ABO_3 perovskite relaxor systems can be broadly classified into three categories: (i) solid-solution systems involving a polar and non-polar material (e.g. $BaTiO_3$: $BaZrO_3$), (ii) polar material incorporated with aliovalent dopant either at A (e.g. $Pb_{1-x}La_x(Zr_yTi_{1-y})_{1-x/4}O_3$) or B site ($Ba(Nb_xTi_{1-x})O_z$), and (iii) complex perovskite oxide compounds with ions with mixed valence at B sites (e.g. $Pb(Mg_{1/3}Nb_{2/3})O_3$, $Pb(Sc_{1/2}Ta_{1/2})O_3$). The common aspect of all the relaxor materials in these three categories is the intrinsic disorder of constituent cations either in A or B site and a broad temperature dependent dielectric anomaly loosely termed as diffused phase transition (DPT). Extensive studies have been made to understand the underlying mechanism of relaxor behavior in various complex perovskite systems (category III) and several models have been proposed to explain the observed relaxor behavior which is summarized as follows: As proposed by Smolenski in case of the ABO_3 perovskite, the diffuse nature of dielectric maxima is related to the cation disorder in the 'B' site of the lattice [21]. This model fails due to the observed fact that many ferroelectrics that exhibit DPT characteristics are not all necessarily exhibit relaxor characteristics. The relaxor nature is proposed to be due to short-range cation order in polar nano-regions in a disorder matrix [22]. In these nano-scale clusters the dipole moments thermally fluctuates between equivalent directions [1]. The broad distribution of relaxation times for cluster orientation originates from the distribution of the potential barriers separating the different orientational states. Each nano-polar region was considered having no interaction among each other and in this respect the material system was considered analogous to super-paramagnetic system and thus the relaxor material system termed as superparaelectric [4]. However, the frequency dispersion of the dielectric maxima (T_m) do not follow a simple Debye type relaxation and in that respect it was postulated that the said polar nano-regions are interactive among themselves unlike the case of a superparamegnetic material [23]. In other words, the relaxors behave like interacting ordered nano-polar regions in a matrix with cation disorder and in this respect the relaxor systems have been proposed to behave like a spin glass state with similar interacting superparamagnetic clusters [24]. In PMN system, a short range cooperative interaction between these superparaelectric clusters was considered by Viehland *et al.* to explain the freezing of the superparaelectric moments into dipolar glassy state with long range polarization ordering at lower temperature [2]. Qian and Bursill [25] on the other hand assumed that the nanometer scale chemical defects are the source of random fields, which control the dynamics of the polar clusters in relaxor systems. The broad dispersive behavior of the temperature dependent dielectric anomaly has been explained by considering changes in the cluster size and correlation length as function of temperature. Despite of extensive studies in last two decades the dielectric relaxation phenomena in bulk relaxor ceramics remain unclear. As compared to category II and III based relaxor systems, the underlying mechanism resulting the relaxation behavior of category I based relaxor systems have been less studied especially in thin film form. The relaxor behavior was in fact first reported by Smolenskii et al in one of such systems namely Sn doped $BaTiO_3$, followed by Hf, Ce, Y, Zr doped $BaTiO_3$ ceramics (beyond a critical dopant contents) have also been reported to exhibit typical relaxor behavior [26].

In the present work the observed relaxor behavior in BZT thin films (with Zr content $\geq$25.0 at%) can be hypothesized as follows: In BZT solid solution system, the B site is randomly occupied by either Ti^{+4} or Zr^{+4} ions. $BaZrO_3$ is cubic and non-ferroelectric whereas $BaTiO_3$ is ferroelectric with tetragonal crystal structure at room temperature. The long-range polarization ordering due to Ti-O dipole-dipole interaction (yielding so called domain structure) in $BaTiO_3$ is hindered due to Zr^{+4} substitution. The primary support of this hypothesis is reflected in the measured room temperature polarization hysteresis as a function of Zr content (Fig. 5). The figure shows that as the Zr contents are systematically increased the hysteresis loops become slimmer which indicates that the long range polarization ordering is broken with Zr doping. From XRD analyses we have found that within the detection limit of the X-Ray diffractometer used, up to 70.0 at%, Zr^{+4} ions are completely soluble in $BaTiO_3$ thin films without the formation of any secondary phase/(s). The solubility of Zr in $BaTiO_3$ lattice has been confirmed by systematic increase of the lattice parameter of BZT films with the increase in Zr contents [9]. Within the limit of this solid solubility, no cationic order between Zr^{+4} and Ti^{+4} cations are expected in $Ba(Zr_xTi_{1-x})O_3$ thin films. The long range polarization order of BTO is marginally disturbed when Zr content is less (say 5.0 at%), however, in case of 20.0 at% Zr doped film, due to the abundance of Zr modified oxygen octahedra the long range periodicity of Ti modified oxygen octahedra is disturbed and the polar regions are developed in a weakly polar matrix. The observed slimmer polarization hysteresis of BZT-20 thin films probably indicates that the dimension of the polar regions are smaller than the size of the micron size domains in BTO thin film, however, they are large enough to have necessary dipolar cooperation among neighboring unit cells to exhibit

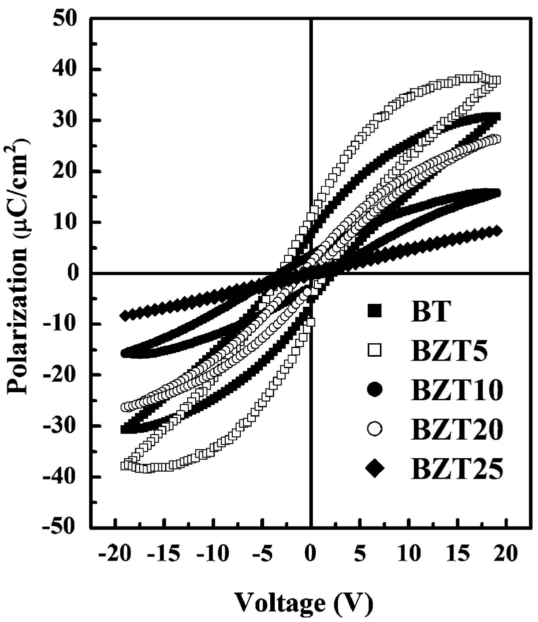

Figure 5 Polarization hysteresis of Ba(Zr$_x$Ti$_{1-x}$)O$_3$ ($0 \leq x \leq 0.25$) thin films measured at room temperature.

polarization hysteresis. With the increase in Zr content the size of the polar regions are decreased and the Zr rich regions are increased and as a result the intermediate layer in the vicinity of the polar regions becomes more and more non-polar. It is noticed that the mode at $\sim$125 cm^{-1} present in all Zr rich (>5.0 at%) BZT thin film of the measured temperature. Smaller the sizes of the PR regions larger are the temperature fluctuations in them [1]. The thermal energy (kT) results the polarization fluctuations in the polar regions. In other words the polarization in these PR are dynamic in nature and the thin film starts behaving like a relaxor. Since, Zr and Ti ions are in same valence state and also the magnitude of their ionic radii are not very different; substitution of Ti by Zr is not expected to yield very strong random field at relatively lower Zr contents. However, a mutual interaction between the polar and non-polar regions is expected and as the fraction of Zr rich regions are increased. The nature of this interaction may be electrostatic or elastic in nature. Unless they are far apart the electrostatic interaction is plausible through dipolar interaction among the PR. Moreover, it has been proposed that PR regions create a complicated pattern of normal and shear strains in the PE surroundings. The mutual interaction among the polar regions depends on their arrangements, spacing, as well as direction of spontaneous polarization in them [27]. The mutual interaction among the polar regions, as well as interaction (electro-static as well as elastic) among the polar regions and non-polar regions could be the source of random field, which becomes significant with the increase of Zr contents. As shown in Table I, the decrease of T_m with the increase of Zr contents could be due to the increase of the magnitude this random field [28]. Additionally, in the case of BZT thin films, microstructure could also induce random field distribution. As for example the grain boundary could contribute random electric field in addition to that produced by the mutual interaction among the polar and non-polar regions. We have observed that the grain size of the BZT film decreases with the increase of Zr contents [15]. Smaller grain size and higher concentration of grain boundary would in turn increase the random field strength and thereby T_m is reduced with the increase in Zr contents. The broadening of the dielectric anomaly could also be related to the relative fraction of the polar regions. As the fraction of the polar regions reduces with the increase of the Zr contents, the broadening (Δ) also decreases (see Table I). The degree of relaxation (γ) is also related to the mean size of the polar regions. As mentioned earlier, with the increase in Zr contents the size of the polar regions are influenced, and γ is maximum at a critical Zr contents of about 40.0 at% and beyond that it decreases as the mean size of the polar regions changes.

The frequency dispersion of the dielectric anomaly of BZT thin films relaxors follow the well-known Vogel-Fulcher relation (Equation 2). In Equation 2, E_a represents the activation energy of the polarization fluctuation. On cooling, the polarization fluctuation minimizes due to the development of short range ordering between the neighboring polar regions. The dispersion of the size of these polar regions decides the spectrum of the relaxation time. With the analogy of a magnetic spin glass system, E_a is believed to be a product of the volume of the polar region (V_{PR}) and the anisotropic energy of polarization direction (K_{anis}). K_{anis} represents the barrier for rotation of the polarization vector between the allowable directions of a specific crystal structure. Assuming K_{anis} does not change significantly for BZT thin film relaxors with varying Zr contents (30.0 to 70.0 at%) the reduction of the activation energy E_a from 50–60 meV (for 30.0 to 40.0 at% Zr doped films) to 20–30 meV (for 60.0–70.0 at% Zr doped films) indicates that the volume content of the polar regions (V_{PR}) reduce with the increase in Zr contents (Table II). As the temperature is reduced a strong correlation among the polar regions may develop which would tend to drive the system towards a long-range ferroelectric state. The parameter kT_f can be considered as a measure of the interaction energy required for the correlation among the polar regions. As shown in Table II, the systematic reduction of T_f (thereby kT_f) probably indicates that the tendency for long range polar ordering reduces in BZT relaxor films with the increase in Zr contents. The order of the pre-exponential factor is about 2–4 orders of magnitude smaller than that reported for PMN bulk relaxor [2]. The difference could be due to difference in sizes and nature of the polar regions in these two systems.

To get further understanding about the nature of the polar regions we have performed detailed analyses of the recorded Raman spectra of BZT thin films. As pre-

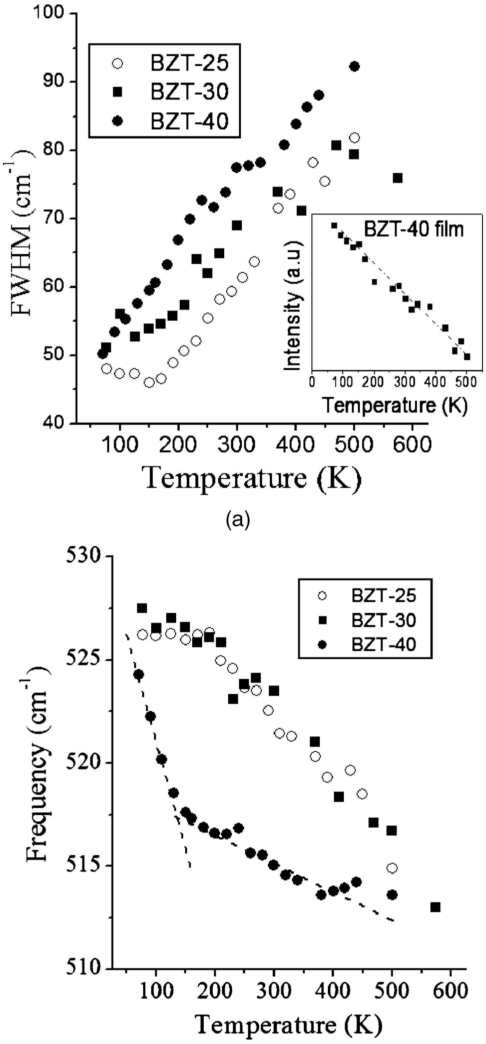

(a)

(b)

Figure 6 The temperature variation of (a) the FWHM and (b) the frequencies of TO mode of BZT thin films with various Zr contents. The inset of Fig. 6a shows the variation of the integrated intensity of TO mode as a function of temperature for BZT 40 thin film.

sented earlier the observed Raman modes in these thin films result from the coupling of the hard phonon polar modes with the fluctuating polarization in the polar regions. For relaxor ceramics such as 9/65/35 PLZT as well as $Ba(Zr_{0.40}Ti_{0.60})O_3$, it was shown that the integrated intensity of TO mode at $\sim$520 cm^{-1} exhibits a continuous increase upon cooling followed by a plateau region where the intensity does not increase upon further cooling. The temperature corresponding to the initiation of this plateau region correlates well with the corresponding freezing temperatures of these relaxors as determined from the Vogel Fulcher analyses. No appreciable change in FWHM as well as frequency of this mode was observed in relaxor BZT ceramics. The increase of the TO mode intensity has been correlated to the size of the polar regions, both in PLZT and BZT relaxor ceramics. We have performed similar analyses in relaxor BZT thin films and the TO mode has been fitted with a damped harmonic oscillator type phonon function corrected for the Bose-Einstein factor. Fig. 6 shows the temperature variation of (a) the FWHM and (b) the frequencies of TO mode of BZT thin films with various Zr contents. The inset of Fig. 6a shows the variation of the integrated intensity of TO mode as a function of temperature for BZT-40 thin film. Several interesting features are apparent from these plots. First, unlike the bulk BZT-40 relaxor, the integrated intensity is continuously increased with the reduction of temperature and no plateau is observed below the characteristic freezing temperature (T_f). Secondly, with the increase in Zr contents ($\geq$25.0 at%), irrespective of the temperature, the magnitudes of FWHM are increased whereas the mode frequencies are systematically decreased. Thirdly, with the decrease in measurement temperature, there is a continuous decrease of the FWHM and increase of the TO mode frequency for all BZT thin film relaxor compositions. The behavior of the fitted TO Raman mode correlates well with the hypothesis presented earlier in this section for BZT relaxor thin films. Thus, the continuous increase of the integrated intensity of the TO mode with the reduction in temperature is indeed related to the growth of polar regions due to increased mutual interaction among them with cooling. For BZT 40 thin films, probably the clustering of the polar regions continue below the freezing temperature yielding a long rage polarization order. The change in the magnitudes of the half width and the mode frequency reflects the size of the polar regions: lower FWHM indicates bigger polar regions whereas bigger the polar regions larger are their mode frequencies. Viewing in this light one can identify that irrespective of the temperature, with the increase in Zr contents the size of the polar regions are continuously reduced and also for all BZT relaxor thin films, the size of the polar regions increases with the reduction of temperature. Although not very prominent in 25.0 and 30.0 at% Zr doped compositions; in case of BZT-40 thin film, a distinct change in the slope of frequency (as marked by dashed lines in Fig. 6b) is apparent. The temperature corresponding to this slope change matches well with the freezing temperature for this composition (see Table II) and the rapid increase of the frequency below the characteristic freezing temperature probably indicates the occurrence of a long range polar ordering below the freezing temperature. Fig. 7 shows the polarization hysteresis of BZT-40 thin films measured at different temperature. The appearance of polarization hysteresis below the characteristic T_f of BZT thin film indeed indicate the induction of long range polar order. It remains unclear whether in relaxor BZT ceramics undergoes a transition from a relaxor phase to a ferroelectric state at T_f [12, 13]. Our data indicates such a transition occurs in BZT-40 thin films.

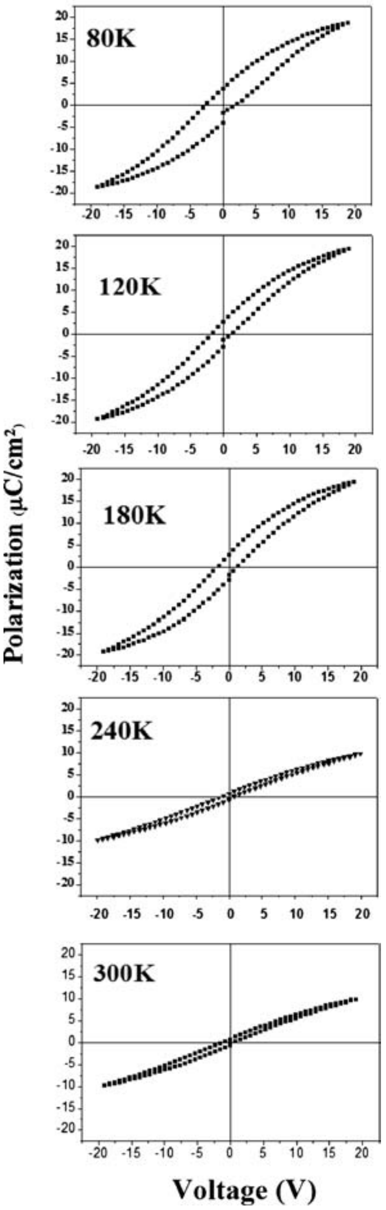

Figure 7 Polarization hysteresis of Ba($Zr_{0.40}Ti_{0.60}$)O_3 thin films measured in the temperature range of 80–300 K.

5. Conclusions

The present work was devoted to understand the relaxor behavior of sol-gel derived Ba(Zr_xTi_{1-x})O_3 (BZT) thin films ($0.30 \leq x \leq 0.70$). Beyond 25.0 at% Zr substitution, BZT thin films exhibit typical relaxor characteristics with a diffuse temperature dependent dielectric anomaly coupled with the shift of both the dielectric constant and loss tangent towards higher temperature with the increase in measurement frequencies. It was found that the temperature corresponding to the peak of dielectric anomaly (T_m) as well as the degree of broadening (Δ) systematically reduced with the increase in Zr content, whereas the degree of relaxation (γ) had a maximum ($\sim$1.8) at 40.0 at% Zr doped BZT film. The long range polarization ordering is disturbed with Zr substitution in Ti site of the barium titanate (BTO) lattice to yield polar region (Ti rich) whose sizes are reduced with the increase in Zr contents. The dielectric relaxation in these thin films is attributed due to the presence of these polar regions in a non-polar host. The frequency dependence of the dielectric anomaly follows Vogel-Fulcher (VF) relation indicating the interaction among these nano-polar regions followed by a cooperative freezing similar to that of spin-glass systems and classic complex oxide relaxor ferroelectrics. The activation energy (E_a) and the freezing temperature (T_f) as a function of Zr contents were estimated from the VF fitting of the dielectric maxima vs frequency data. From the fact that both E_a and T_f reduce with the increase in Zr contents, it has been argued that the volume of the polar regions and the interaction energy for cooperative freezing reduce with the increase in Zr contents. The existence of these polar regions is ascertained on the basis of the analyses of micro-Raman spectra. The temperature dependent Raman spectra indicated a rhombohedral structure of these polar regions (irrespective of the Zr contents) at liquid nitrogen temperature and no apparent structural transition was observed upon heating far above the temperature corresponding to the dielectric maxima (T_m). From the variation of the frequency and the full width at half maxima of the TO mode of Raman spectra for relaxor BZT films it was supported that (i) with the increase of Zr contents the size of the polar regions are reduced and (ii) when Zr content is fixed, the size of the polar regions increase with cooling yielding a long range polar ordering. Thus, in case of BZT-40 thin film, a stable polarization hysteresis was obtained below its freezing temperature. Detailed micro-Raman analyses in conjunction with temperature dependent transmission electron microscopy measurements are in progress to further investigate the relaxor behavior in these films.

Acknowledgements

This work was supported in parts by NSF-DMR 305588 and NSF-ID 100097018 grants.

References

1. L. E. CROSS, *Ferroelectrics* **76** (1987) 241.
2. D. VIEHLAND, S. J. JANG, L. E. CROSS and M. WUTTIG, *J. Appl. Phys.* **68** (1990) 2916.
3. V. WESTPHAL, W. KLEEMANN and M. D. GLINCHUK, *Phys. Rev. Lett.* **68** (1992) 847.
4. L. E. CROSS, *Ferroelectrics.* **151** (1994) 305.
5. G. A. SAMARA, *J. Phys.: Condens. Matter.* **15** (2003) R367.
6. Z. YU, C. ANG, R. GUO and A. S. BHALLA, *J. Appl. Phys.* **92** (2002) 2655.
7. Idem. *ibid.*, **92** (2002) 1489.
8. Z. YU, R. GUO and A. S. BHALLA, *ibid.* **88** (2000) 410.

9. A. DIXIT, S. B. MAJUMDER, R. S. KATIYAR and A. S. BHALLA, *Appl. Phys. Lett.* **82** (2003) 2679.
10. J. ZHAI, X. YAO, L. ZHANG and B. SHEN, *ibid.* **84** (2004) 3136.
11. P. SCIAU and A. M. CASTAGNOS, *Ferroelectrics,* **270** (2002) 259.
12. P. SCIAU, G. CALVANIN and J. RAVEZ, *Solid State Comm.* **113** (2000) 77.
13. R. FARHI, M. E. MARSSI, A. SIMON and J. RAVEZ, *J. Eur. Phys. B* **9** (1999) 599.
14. Y. HOTTA, G. W. J. HASSINK, T. KAWAI and H. TABATA, *Jpn. J. Appl. Phys.* **42** (2003) 5908.
15. A. DIXIT, S. B. MAJUMDER, A. SAVVINOV, R. GUO and A. S. BHALLA, *Mat. Lett.* **56** (2002) 933.
16. H. T. MARTIRENA and J. C. BURFOOT, *Ferroelectric.* **7** (1974) 151.
17. G. BURNS and F. H. DACOL, *Phys. Rev. B.* **28** (1983) 2527.
18. H. VOGEL, *Z. Phys.* **22** (1921) 645; G. FULCHER, *J. Am. Ceram. Soc.* **8** (1925) 339.

19 A. DIXIT, S. B. MAJUMDER, P. S. DOBAL, R. S. KATIYAR and A. S. BHALLA, *Thin Solid Films* **447–448** (2004) 284.

20. I. G. SINY, R. S. KATIYAR and A. S. BHALLA, *Ferroelectric Review.* **2** (2000) 51.
21. G. SMOLENSKI and A. AGRANOVSKAYA, *Sov. Phys. Solid State.* **1** (1960) 1429.
22. C. RANDALL, A. BHALLA, T. SHROUT and L. E. CROSS, *J. Mater. Res.* **5** (1990) 829.
23. L. NEEL, *Compt Rend. Acad. Sci.* **228** (1949) 664.
24. A. MORGONWNIK and J. MYDOSH, *Solid State Commun.* **47** (1983) 321.
25. H. QIAN and L. A. BURSILL, *Int. J. Mod. Phys. B* **10** (1996) 2007.
26. C. ANG, Z. JING and Z. YU, *J. Phys. Condens. Matter.* **14** (2002) 890 and references therein.
27. V. A. ISUPOV, *Physics of the Solid State* **45** (2003) 1107.
28. M. D. GLINCHUK and R. FARHI, *J. Phys.: Condens. Mater* **8** (1996) 6985.